Research Article

Wei Chen, Gaiyan Yang*, Liguang Zhu, Xingjuan Wang, and Baomin He

Reducing Surface Cracks and Improving Cleanliness of H-Beam Blanks in Continuous Casting — Improving continuous casting of H-beam blanks

https://doi.org/10.1515/htmp-2019-0012
Received Jul 27, 2018; accepted Dec 03, 2018

Abstract: A beam blank is ideal for H-beam production, but there are more defects in/on beam blanks than other common blanks. The study of the H-beam blank quality assurance system has great significance for production to determine the key factors causing defects and optimise the casting process parameters. Experimental analysis and numerical simulation, based on an actual production process, were used as research methods. The former was used to test and analyse the cracks, inclusions, and the flux in the mould to determine the preliminary factors causing defects in a beam blank. The latter was used to simulate the flow and temperature fields and the movement of inclusions to determine the key factor leading to defects and to optimize the casting process parameters. Online implementation of the recommendations of this project was developed, which proved that it is very useful and efficient to control surface cracks on the web and enhance cleanliness of an H-beam blank.

Keywords: H-beam blank; continuous casting; surface cracks; cleanliness; quality control

1 Introduction

H-beam steel is an economic type of sectional material that has been widely used in many fields of construction [1, 2]. A near-net-shape casting beam blank is ideal for producing H-beam steel. At present, there are only a small number of production lines for beam blanks in China. Such blanks have more internal and surface defects than other common strands, due to their complex cross-section and many difficult engineering and operating problems [3–5].

Unfortunately, little information is available in the literature concerning beam blank casting. Kim developed a two-dimensional (2D) transient-coupled thermal–elastic–plastic finite-element model (FEM) to analyse surface and internal cracks in a continuously cast beam blank [6]. Jung-Eui built a three-dimensional (3D) mathematical model to analyse continuous beam blank casting using body-fitted coordinates [7]. Luo Wei established a thermal–mechanical model for a copper plate mould using *ABAQUS* software to analyse the temperature and stress distributions of the mould and strand and the air gap between the solidified shell and mould [8]. According to the deformation of a copper plate mould and beam blank, Shen Quan proposed the concept of tapered optimization for each side [9]. A 3D flow field model for a beam blank mould was built by our team to optimize flow behaviour and accelerate inclusion removal [10], and a thermal–mechanical model was proposed to optimize the second cooling system [11, 12]. Although these efforts have resulted in many benefits to beam blank production, such studies are usually based on only a single process or defect, rather than the entire continuous casting production process. It remains necessary to study the control of steel quality, to determine the key factors causing defects, and to optimize the entire continuous casting process.

Based on the actual process used at Hebei Jinxi Iron & Steel Co., Ltd., China, this study aimed to determine the key factors causing surface cracks and cleanliness defects

***Corresponding Author: Gaiyan Yang:** North China University of Science and Technology, Tangshan 063210, Hebei, China; Hebei Engineering Research Center of High Quality Steel Continuous Casting, Tangshan 063009, Hebei, China; School of Metallurgical and Ecological Engineering, University of Science and Technology Beijing, Beijing, 100083; Email: gaiyanyang-1@163.com; Tel.: +8615032906094

Wei Chen, Liguang Zhu, Xingjuan Wang, Baomin He: North China University of Science and Technology, Tangshan 063210, Hebei, China; Hebei Engineering Research Center of High Quality Steel Continuous Casting, Tangshan 063009, Hebei, China

in beam blanks and to optimize the casting process. Two research methods were employed, *i.e.*, experimental analysis and numerical simulation. The former was used to test and analyse the cracks, inclusions, and the flux in the mould, and hence determine the preliminary factor causing defects of a beam blank. The latter simulated the flow field, temperature field, and the movement of inclusions to determine the key factor that leads to defects and thereby optimize the casting process parameters.

2 Experimental Analysis

2.1 Observation and analysis of cracks in H-beam web

The production line for beam blanks in this corporation comprises the following sequential steps in the transfer of the steel: hot metal pretreatment → converter → tundish → continuous caster → hot charging → rolling. When the caster was first put into production, some defects appeared in and on H-beam blanks, such as longitudinal surface cracks, pinholes, cinder inclusions, and scratches. In particular, a 5% H-beam blank web with longitudinal cracks would result in outside grinding in the subsequent hot-rolling step; in the worst situations, the strands would become useless. Figure 1 shows macroscopic features of longitudinal cracks on the surface of a beam web.

Figure 1: Cracks on web of H-beam.

To analyse the microscopic cracks, a number of test samples with a length of 100 mm were cut at the crack zones. After being roughly ground, finely ground, burnished, and numbered, the samples were observed and analysed using a metallographic microscope (Leica DM6M, Germany), scanning electron microscope (S-4800 SEM, Hitachi, Japan), and energy-dispersive spectrometer (EDS, NORAN7, ThermoFisher, USA). The constitution diagrams showed that these cracks were wide, generally 0.5–1.5 mm, and of regular shape, most of which were in the shape of a long strip. The cracks had an inward extension. Normally, if cracks appear in a rolling process, they are shallow, parallel to the web surface, and have no inward extension; therefore, it was concluded that these cracks resulted from the continuous casting process, rather than the rolling process. In stereoscan photographs, oxide particles were found close to the cracks, which indicated that the cracks appeared at a high temperature. Energy spectrum analyses showed that there was a greater concentration of impurity elements, such as Al, Ca, Si, Mn, and K, in the crack region. There was a high content of inclusions of many types. Analysis of the steel components showed that its cleanliness was low and that the sulphur content could be as high as 0.059%.

2.2 Analysis of cleanliness of beam blank

To analyse the cleanliness of the beam blank, a tracer method, systematic sampling, and comprehensive analysis were used. The tracer method aimed to investigate the origin of different inclusions by adding tracers of Ba, La, Ce, K (or Na) into the ladle slag, the tundish covering flux, the tundish lining, and the mould powder, respectively. The systematic sampling procedure involved taking samples from the converter, tundish, mould, casting billet, and milled bar. For the comprehensive analysis, the content of oxygen in each sample was assayed by infrared absorption (VERTEX70, Bruker, Germany), the content, feature, size, and principal origin of large-scale inclusions was analysed by electrolyzing the samples and stereoscanning, and the amount, shape, size, distribution, and origin of micro-inclusions was analysed by metallographic microscope and stereoscanning [13, 14]. The concentration of each element in the inclusions was determined from an energy spectrum analysis.

According to the results of the infra-red absorption analysis, the total oxygen concentrations (T[O]) in the steel were 0.0957% in the ladle and 0.0986%–0.0939% in the tundish under conditions of steady-state casting, but increased to 0.140% in the mould. T[O] was 0.067% in the billet. Therefore, the oxygen content was higher during all of the processes, which indicated that the content of inclusions was higher. The type and origin of the inclusions in all the process steps was therefore analysed.

According to the results of the sample-electrolysis analysis, the average contents of large-scale non-metallic inclusions were 108.79 mg/10 kg in the tundish under conditions of steady-state casting and 78.75 mg/10 kg in the

Table 1: Energy spectrum analysis of chemical composition of inclusion shown in Figure 2.

Component	Si	Al	Ca	Fe	S	Mn	Mg	Ti	Na/K
Wt (%)	14.95	3.35	11.54	3.03	0.63	8.69	5.02	10.99	0.43/0.99

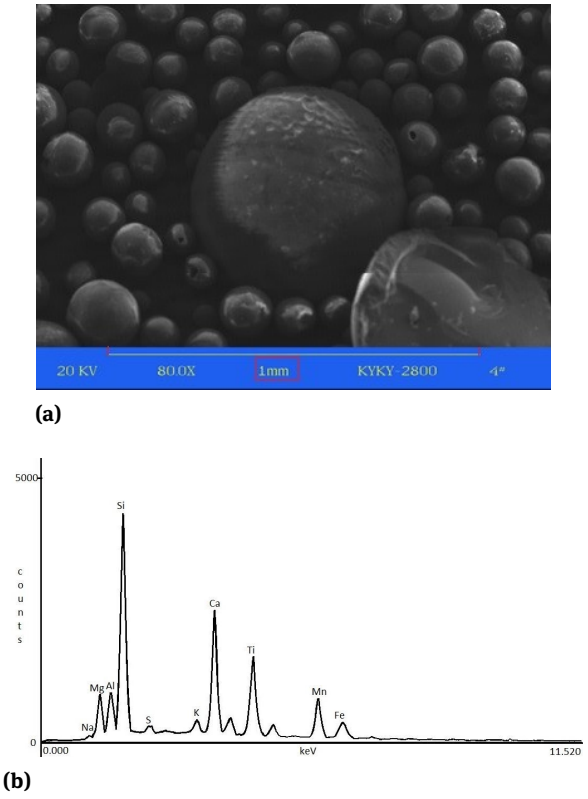

Figure 2: (**a**) Stereoscan photograph and (**b**) energy spectrum analysis of SiO_2–CaO–MnO–MgO–TixOy impurity.

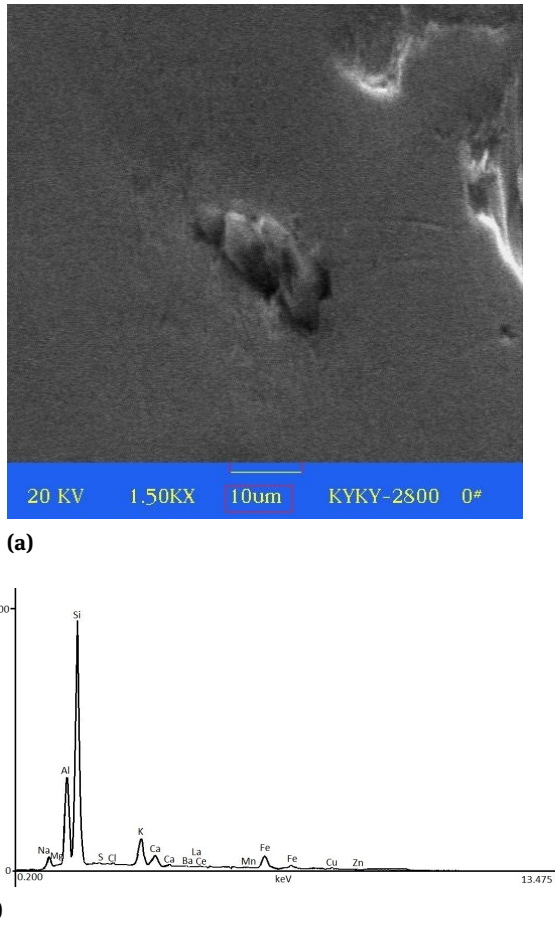

Figure 3: (**a**) Stereoscan photograph and (**b**) energy spectrum analysis of silicon–alumina duplex impurity.

billet. The inclusions in the tundish included many complex components, such as CaO, SiO_2–Al_2O_3, SiO_2–CaO, SiO_2–CaO–MgO–Al_2O_3, and SiO_2 particles. Figure 2 and Table 1 show a stereoscan photograph (Figure 2a) and energy spectrum analysis of a SiO_2–CaO–MnO–MgO–TixOy impurity (Figure 2b, Table 1). All inclusions in the tested samples contained the Ba tracer, which indicated that the inclusions originated from the ladle slag and were not totally removed in the tundish. Some 75% of the inclusions in the tested samples contained the La tracer, indicating that inclusions also came from the tundish covering flux. The Ce tracer was found in 62.5% of the inclusions, indicating that they originated from the tundish lining. The inclusions in the strand were complex, including those of SiO_2–CaO–MnS–Al_2O_3, SiO_2–CaO–Al_2O_3, CaO–CaS, SiO_2–CaO–MnO–MgO–Al_2O_3, and SiO_2–Al_2O_3. Inclusions containing Ba, La, and Ce accounted for 66.7%, 38.9%, and 27.8% of the total tested samples, respectively; all samples contained the K (or Na) tracer.

The micro-inclusion tests indicated that their size in the strand was small: inclusions ranging from 0–10 μm in diameter comprised 64% of the total inclusions and only 20% were larger than 20 μm. The volume percentage of all types of micro-inclusions was about 0.15%. The percentage of inclusions decreased from the internal to the external arc strand. Moreover, the micro-inclusions were enriched in the centre of the strand. Three types of micro-inclusion components were identified: globular calcium silicate inclusions, aluminosilicate inclusions, and spheric sulfide inclusions. Figure 3 shows a stereoscan

Table 2: Basicity and chemical composition of mould slag.

	R	SiO_2 (%)	CaO (%)	Al_2O_3 (%)	Fe_2O_3 (%)	C (%)	H_2O (%)
HDK-2	0.86	29-30	25-26	10-11	3-3.5	15-17	≤ 0.5

photograph (Figure 3a) and energy spectrum (Figure 3b) of a silicon–alumina duplex impurity.

2.3 Analysis of physical and chemical indices of mould slag

The mould slag used in production is HDK-2 type, produced by Xibao, China. Its basicity and chemical composition are shown in Table 2. The melting temperature and time of the slag were studied by means of a fully automatic determinator. The average melting temperature and melting time were 1440 K and 57 s, respectively; the viscosity of the slag was 0.77 Pa·s.

The optimal melting temperature of a mould slag should generally be 50 K lower than that of the shell at the end of the mould; however, the temperature of this slag was 34 K higher than that of the shell. A high melting temperature results in insufficient melting of the slag film between the solid shell and copper wall, which could cause poor lubrication and heat transfer of the slag in the mould. As a result, the probability of surface defects of the strand would increase, and breakout accidents could even occur. Comparison with the optimal melting time for Q235 steel (30–40 s) indicated that this mould slag was slow melting (57 s), so it was difficult to control the ideal thickness of 7–12 mm of the molten slag layer. Generally, the viscosity of a mould flux should be controlled in the range of 0.3–0.6 Pa·s for a small beam blank at a pulling rate of 0.9–1.1 m/min. It was clear that the viscosity of this mould slag was higher than optimum.

3 Numerical Simulation

3.1 Numerical simulation of flow field of molten steel in tundish

The tundish is the key equipment component used to prevent slag from entering the mould, removing non-metallic inclusions, and controlling the temperature of the molten steel. In this study, the 3D coupled flow and temperature fields in the tundish were simulated by using an FEM. The movement of inclusions, their collection rate from the outlets, and removal rates were calculated, and the shortcomings of the fluid flow in the tundish analysed. Moreover, to increase the cleanliness of the steel, the structure of the turbulence inhibitor was optimised. The structure of the tundish and designs of two turbulence inhibitors are shown in Figure 4. The velocity vectors and temperature distributions of the two tundishes are shown in Figures 5 and 6, respectively. Figure 7 shows the trajectory of inclusions in the tundish with turbulence inhibitor B.

According to the results of this analysis, the tundish A that used the turbulence inhibitor A could not eliminate short-circuit flow due to the lower short-dam of this turbulence inhibitor. The temperature difference between each outlet ranged from 6 to 8 K. The difference in the inclusion collection between 1# and 2# outlets was 7% and the average inclusion removal efficiency was 60%.

The flow features of tundish B that used the optimized turbulence inhibitor B was better: short-circuit flow was eliminated and the temperature throughout the entire tundish was homogenous. The temperature difference between the outlets was less than 4 K, which was a drop of 2–4 K compared with that in tundish A. The difference in the inclusion collection between 1# and 2# outlets was less than 2%, representing a decline of 5% compared with tundish A. The average inclusion removal was 58% – a drop of 2% compared with tundish A.

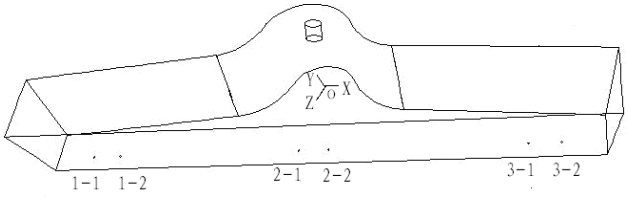

(a) Structure of tundish

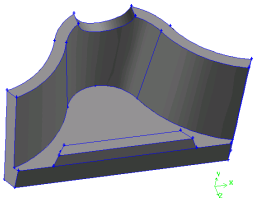

(b) A turbulence inhibitor

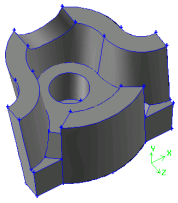

(c) B turbulence inhibitor

Figure 4: Structures of tundish and designs of two turbulence inhibitors.

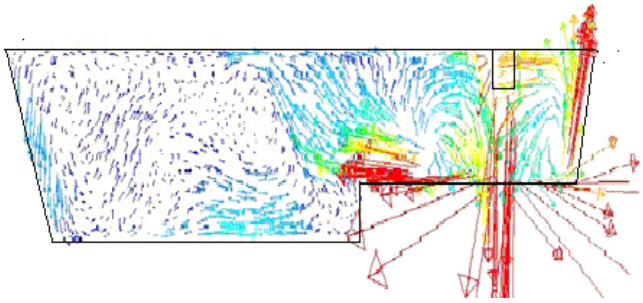

(a) A tundish

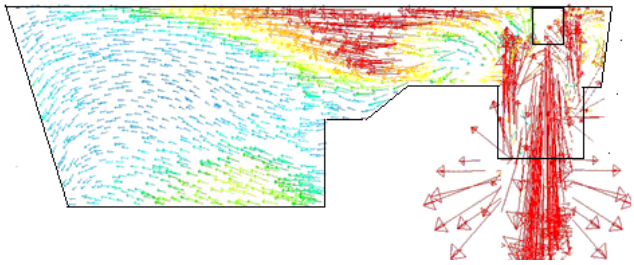

(b) B tundish

Figure 5: Velocity vectors in tundish.

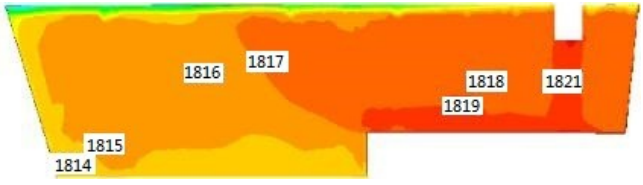

(a) A tundish

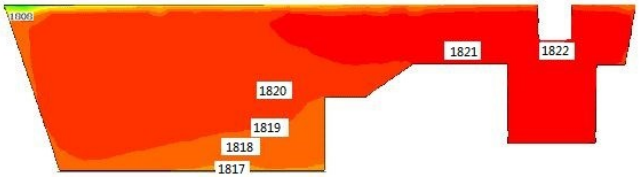

(b) B tundish

Figure 6: Temperature distribution in tundish.

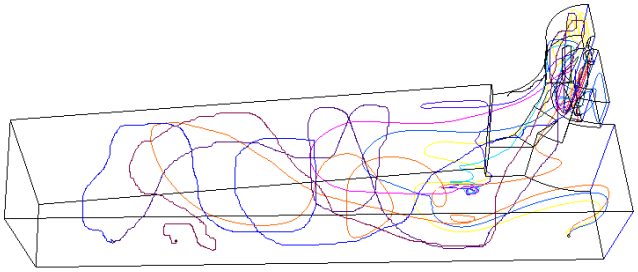

Figure 7: Trajectory of inclusions in tundish with turbulence inhibitor B (d = 60 m).

In practical production, an unreasonable structure design can lead to the deterioration of molten steel flow, the occurrence of short-circuit flow, and an imbalanced distribution of inclusions at each outlet, which would restrict the flotation and removal of inclusions and thereby strongly affect the cleanliness of the molten steel and beam blank. Therefore, comparison of the flow characteristics of tundishes A and B indicated that the turbulence inhibitor A used in current production should be replaced by the turbulence inhibitor B proposed by these calculations.

3.2 Numerical simulation of molten steel flow in mould

The mould is the last process unit that can control cleanliness of the molten steel. The removal of inclusions and entrainment of mould slag are significantly influenced by the flow of molten steel. The 3D flow field and meniscus fluctuation in the mould were simulated using FEM. The influences of process parameters (such as casting speed and nozzle parameters) on the molten steel flow (such as the location of the vortex, the steel impact depth, and the velocity and fluctuation of the liquid at the free surface) were analysed. To improve cleanliness of the steel, optimum processing parameters were proposed based on these calculations.

The cross-sections of a beam blank and submerged entry nozzle (SEN) and the fluid flow at the flange of the beam blank are shown in Figures 8 and 9, respectively. The simulated results indicated that, if the through-conduit SEN was used under the conditions of the current process, the impacted depth of the main flow was in the range of 1.01–1.16 m and the height of the vortex centre was in the range of 0.5–0.6 m. The oscillation amplitude of the free surface at the flange was around 2.2 mm, but only about 0.8 mm at the web. Therefore, a too large impacted depth of molten steel and a too low vortex centre were disadvantageous for flotation and removal of inclusions, which would affect the cleanliness of the molten steel. Moreover, a small oscillation amplitude of the free surface restricted melting of the mould slag and then weakened its ability to absorb inclusions, thereby significantly influencing the cleanliness of the molten steel.

Analysis indicated that an SEN with a three-side outlet should be adopted, if possible. If the through-conduit SEN was still used, the inserted depth and casting speed should be around 50 mm and larger than 0.9 m/min, respectively, otherwise the meniscus would be too steady; the casting speed should, however, be less than 1.3 m/min, otherwise the meniscus fluctuation would be too strong.

Table 3: Comparison of water consumption before and after optimization.

	Spray 1	Spray 2	Former Spray 3	Latter Spray 3	Spray 4	Spray 5	Total
Initial water consumption (m^3/min)	0.253	0.188	0.057	0.057	0.047	0.021	0.623
Optimized water consumption by MOGA combined with the FEM (m^3/min)	0.233	0.175	0.058	0.052	0.015	0.006	0.539

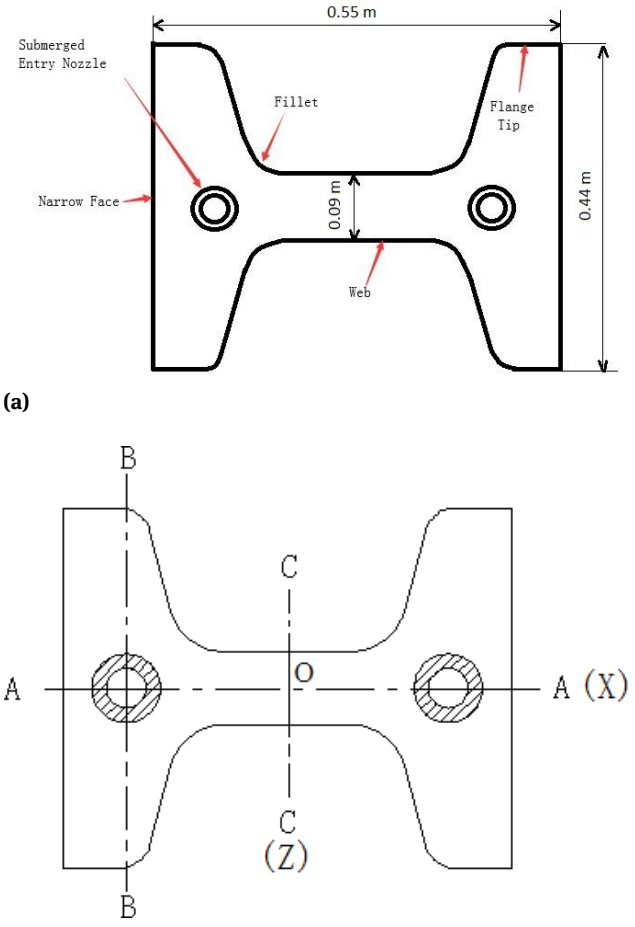

Figure 8: Cross-section of beam blank and submerged entry nozzle.

3.3 Simulation and optimization of solidification process of beam blank

The solidification and cooling of molten steel play a critical role in the quality of a beam blank because its continuous casting is a very complex, high-temperature process. A coupled 2D thermal–mechanical FEM was developed to calculate the temperature and stress–strain fields in the beam blank. By comparing the calculated data with the metallurgical constraints, the key factors causing cracks on the beam blank could be determined. A new optimization method was developed to optimize the process parameters, which combined a MOGA (multi-objective genetic algorithm) with the FEM: dynamic invocation and calculation between the two procedures were repeatedly carried out. In this method, FEM (based on *ANSYS* software, USA) was used to calculate the thermal–mechanical fields for beam blank continuous casting and the MOGA (based on *MATLAB* software, USA) was used to find the optimum process parameters according to the FEM results and metallurgical constraints. The optimum parameters should meet all specific requirements with minimum operational cost and within design constraints, and make it possible to run the caster at maximum productivity and minimum cost to cast defect-free products.

Figure 10 shows the FE grids and some representative points on the beam blank cross-section. Figure 11 shows the calculated temperature as a function of time at different positions from the mould to the air-cooling zone. The calculated results demonstrated that the key factor that caused surface cracks on the web was that the heat flow density was much too high. High heat flow caused the temperature in the straightening zone to be lower than the constraint temperature; moreover, the surface temperature caused great fluctuations on the transverse web, so the stress and strain exhibited quite high values in this region. In the centre of the surface web, the temperature was only 1053 K at the straightening zone, which was just on the point of critical lowest plasticity. The temperature increased by 120 K from the centre to the edge of the web, which was expected to induce great tensile stress. Therefore, when the strand passed the straightening zone, surface cracks could occur on the web under the influence of this unbending force and the poor cleanliness of the steel.

To avoid the formation of surface cracks on the web, the cooling system was modified using the MOGA optimization method combined with the FEM. Comparison of the water consumption before and after optimization is shown in Table 3. Figures 12 and 13 show comparisons of initial and optimized temperature and stresses on the surface web, respectively. The optimized temperature at the unbending zone was in the range of 1109–1181 K on the surface web, which is higher than the limit of the ductility

trough. The curves of the optimized surface temperature and stress are smoother than those of the initial conditions, which implies less possibility of generating surface cracks.

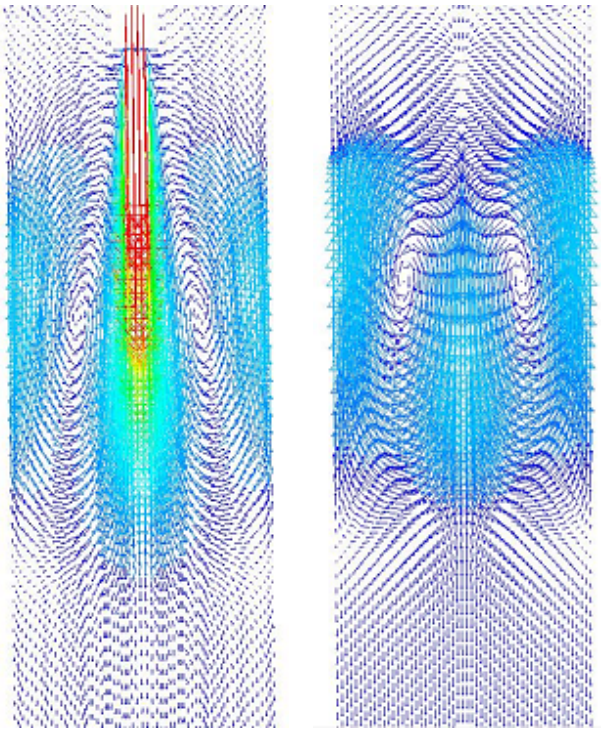

(a) B-B section **(b)** Near the beam blank flange

Figure 9: Fluid flow at flange of beam blank.

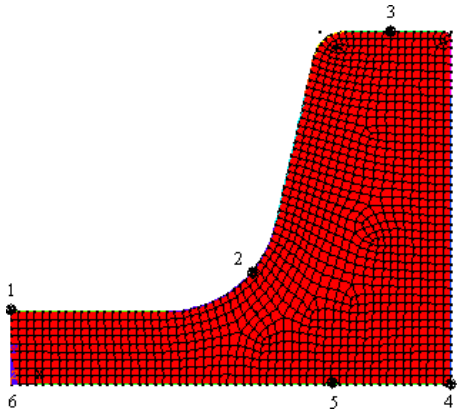

Figure 10: Finite-element grids and some representative points.

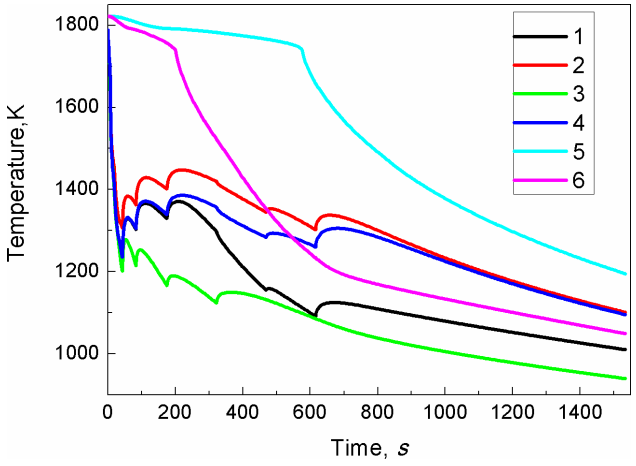

Figure 11: Temperature as a function of time at different positions.

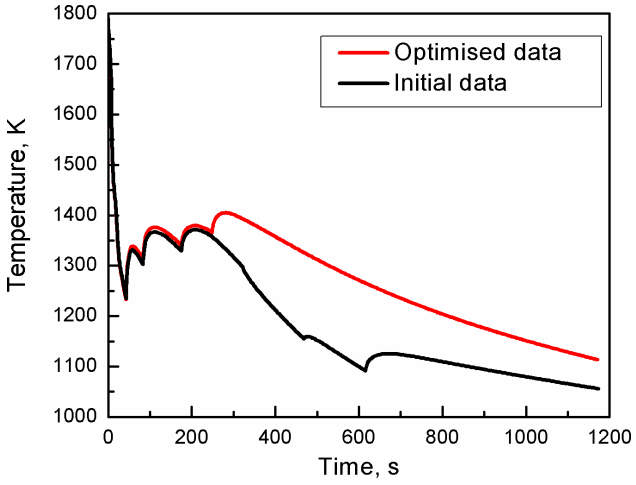

Figure 12: Comparison of initial and optimized temperatures on surface web.

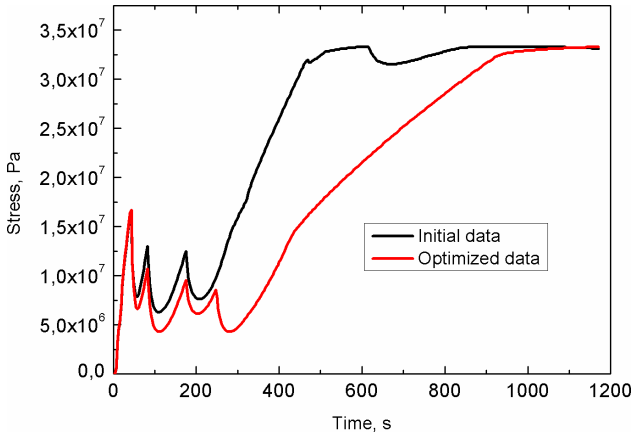

Figure 13: Comparison of initial and optimized stresses on surface web.

4 Measures for Improving Quality of Beam Blank

Comprehensive analysis indicated that (i) the poor cleanliness of the beam blank provided the opportunity for occurrence of defects, such as surface cracks, (ii) the poor physical and chemical performance of the mould slag promoted surface defects in the mould, and (iii) unreasonable flow and temperature fields in the tundish and mould restricted the flotation and removal of inclusions. Therefore, initial cracks that occurred in the mould readily intensified due to the complex surface temperature field in the second cooling zone and new surface cracks would occur. To improve the quality of beam blanks, a series of improvements should be adopted:

(1) Steel cleanliness from the converter should be improved. This can be achieved by, inter alia, reducing the terminal oxygen content by decreasing the amount of slag, enhancing the MgO and Mn/Si contents of the slag, reducing sulfide inclusions by slag-filtrating desulfurization, adding a refining process (such as vacuum argon stirring, powder spraying, or inclusion degenerating), preheating the tundish more precisely, adding a low-carbon flux into the tundish, using a basic refractory tundish lining, or employing a protective casting process [15–18].
(2) The performance of the mould slag can be enhanced by adjusting and improving the function of the flux based on the grade of steel, casting speed, mould amplitude, and cross-section of beam blank.
(3) The structure of the inhibitor in the tundish could be adjusted. The turbulence inhibitor A used in current production should be replaced by that of design B, proposed by calculation, which would not only improve the flow field and temperature distribution of the molten steel, but also enhance the removal of inclusions.
(4) The flow field of the molten steel in the mould should be improved. A SEN with a three-side outlet should be adopted, if possible. If the through-conduit SEN is used, the inserted depth should be around 50 mm and the casting speed between 0.9 and 1.3 m/min for optimum meniscus fluctuation.
(5) Cooling parameters of the second cooling zone should be optimized by restricting cooling water from the third segment into the second cooling zone on the web, using the optimized water consumption so as to reduce the cooling rate, increasing the web temperature and decreasing water consumption, and, if possible, adopting multiple-point instead of single-point straightening.

Online implementation of the recommendations of this project was developed. The probability of surface cracks has been reduced from 5% to 0.5%, which proves that these improvements are very useful and efficient to control surface cracks on the web and enhance cleanliness of the H-beam blank. Moreover, the water consumption of the secondary cooling zone was reduced by 13.4%. This optimum system made it possible to run the caster at maximum productivity and minimum cost and to cast defect-free products.

5 Conclusions

(1) A comprehensive and systematic analysis of the entire beam blank production process was carried out, from converter steelmaking → tundish → continuous caster, with the objective of controlling surface cracks and increasing the cleanliness of H-beam blanks.
(2) Experimental analyses, including study of the cracks, use of a tracer method, systematic sampling, and comprehensive analysis, were carried out. The type, origin, composition, and evolution of inclusions in each step of the beam blank production process were researched. Preliminary factors affecting cleanliness and causing defects of the beam blank were identified.
(3) Numerical simulation, including that of the flow field, temperature field, and movement of inclusions in the tundish, mould, and second cooling zone, were carried out. The key factor causing defects was identified and the optimum casting process parameters determined.
(4) Online verification and implementation of the recommendations of this project were developed, proving that these methods are very useful and efficient to control surface cracks on the web and enhance the cleanliness of H-beam blanks.

Acknowledgement: We thank Kathryn Sole, PhD, from Liwen Bianji, Edanz Group China (www.liwenbianji.cn/ac), for editing the English text of a draft of this manuscript.We also acknowledge the support afforded by the National Natural Science Foundation of China (51574103, 51574106 and 51404088).

References

[1] M.G. Xu and M.Y. Zhu, ISIJ Int., 55(2015) 791-798.
[2] H.L. Xu, G.H. Wen, W. Sun, K.Z. Wang, and B. Yan, J. Iron Steel Res. Int., 17 (2010) 17-22.
[3] J.E. Lee, T.J. Yeo, O.H. Kyu Hwan, J.K. Yoon, and U.S. Yoon, Metall. Mater. Trans. A, 31 (2000) 225–237.
[4] G.Y. Yang, L.G. Zhu, W.Chen, X.W. Yu, G.X. Guo, Metals, 8 (2018) 712.
[5] X.P. Zhang and A.S. Liang, Technique of near shape casting, Metallurgical industry press, Beijing, (2001).
[6] K. Kim, H.N. Han, T. Yeo, Y. Lee, K.H. Oh, and D.N. Lee, Ironmaking Steelmaking, 24 (1997) 249-256.
[7] J.E. Lee, J.K. Yoon, and H.N. Han, ISIJ Int., 32 (1998) 132-141.
[8] W. Luo, Doctoral thesis, Chongqing University, Chongqing, China, (2012).
[9] Q. Shen, Master's thesis, Yanshan University, Qinhuangdao, China, (2013).
[10] W. Chen, Y.Z. Zhang, C.J. Zhang, L.G. Zhu, S.M. Wang, B.X. Wang, J.H. Ma, and W.G. Lu, Ironmaking Steelmaking, 35 (2008) 129-136.
[11] W. Chen, Y.Z. Zhang, C.J. Zhang, L.G. Zhu, W.G. Lu, B.X. Wang, and J.H. Ma, Mater. Sci. Eng. A, 499 (2009) 58-63.
[12] W. Chen, Y.Z. Zhang, L.G. Zhu, C.J. Zhang, Y. Chen, B.X. Wang, and C. Wang, Ironmaking Steelmaking, 39(2012), 560-567.
[13] Y.S. Wang and P.Y. Fu, Shanxi Metallurgy, 4 (1999) 14-15.
[14] J. Zhai, W. Wu, W. Wu, Y.H. Zhou, Y.C. Xiong, B. Hu, Iron Steel, 44 (2009) 98-102.
[15] X.D. Xie, B.H. Zhao, J.Z. Li, and G.W. Chen, Steelmaking, 25 (2009) 37-39.
[16] Y. Zou, Z.X. Yu, and L. Wang, Proceedings of the VII National Conference on Steel Rolling Production Technology, July 23-25, 2002, Benxi iron and steel, China metal society, Liaoning, (2002), pp. 28-36.
[17] X.H. Wang, Iron Steel, 34 (1999) 367-372.
[18] L.G. Zhu and G.M. Di, Hebei Metallurgy, 6 (1998) 4-8.